

Published in final edited form as:

*Anal Biochem.* 2007 July 15; 366(2): 156–169. doi:10.1016/j.ab.2007.04.009.

## Subcellular proteomics of mice gastrocnemius and soleus muscles

Rui Vitorino<sup>a,b</sup>, Rita Ferreira<sup>b</sup>, Maria Neuparth<sup>b</sup>, Sofia Guedes<sup>a</sup>, Jason Williams<sup>c</sup>, Kenneth B. Tomer<sup>c</sup>, Pedro M. Domingues<sup>a</sup>, Hans J. Appell<sup>d</sup>, José A. Duarte<sup>b</sup>, and Francisco M.L. Amado<sup>a,\*</sup>

<sup>a</sup>Department of Chemistry, University of Aveiro, 3810-193 Aveiro, Portugal

<sup>b</sup>CIAFEL, Faculty of Sport, University of Porto, 4200-450 Porto, Portugal

<sup>c</sup>Laboratory of Structural Biology, National Institute of Environmental Health Sciences, National Institutes of Health, Research Triangle Park, NC 27709, USA

<sup>d</sup>Department of Physiology and Anatomy, D-50927 Cologne, Germany

### Abstract

A proteomics characterization of mice soleus and gastrocnemius white portion skeletal muscles was performed using nuclear, mitochondrial/membrane, and cytosolic subcellular fractions. The proposed methodology allowed the elimination of the cytoskeleton proteins from the cytosolic fraction and of basic proteins from the nuclear fraction. The subsequent protein separation by two-dimensional gel electrophoresis prior to mass spectrometry analysis allowed the detection of more than 600 spots in each muscle. In the gastrocnemius muscle fractions, it was possible to identify 178 protein spots corresponding to 108 different proteins. In the soleus muscle fractions, 103 different proteins were identified from 253 positive spot identifications. A bulk of cytoskeleton proteins such as actin, myosin light chains, and troponin were identified in the nuclear fraction, whereas mainly metabolic enzymes were detected in the cytosolic fraction. Transcription factors and proteins associated with protein biosynthesis were identified in skeletal muscles for the first time by proteomics. In addition, proteins involved in the mitochondrial redox system, as well as stress proteins, were identified. Results confirm the potential of this methodology to study the differential expressions of contractile proteins and metabolic enzymes, essential for generating functional diversity of muscles and muscle fiber types.

### Keywords

Skeletal muscle; Subcellular fractionation; Proteomics

---

Human skeletal muscle is very heterogeneous in composition, being constituted by different types of muscle fibers showing significant differences in their contractile speed and metabolic profile that result from specific protein expression [1–4]. In rodents, especially mice and rats, muscle fibers present a more uniform distribution among the different muscles, allowing the use of the entire muscles to study specific phenotypes. In this regard, the soleus and the white portion of gastrocnemius of mice are composed mainly of fast- and slow-twitch muscle fibers, respectively [5–7], and these two muscles have been used as typical models in proteomics.

---

\*Corresponding author. Fax: +351 234370084. E-mail address: famado@dq.ua.pt (F.M.L. Amado).

During the past few years, several studies have been performed using two-dimensional gel electrophoresis (2-DE)<sup>1</sup> combined with mass spectrometry (MS) to characterize skeletal muscle protein composition of typical slow- and fast-twitch skeletal muscles [8–17]. In a recent proteomics study on murine gastrocnemius and soleus muscle extracts, performed by Gelfi and coworkers [9], more than 800 spots on each 2-DE were detected by silver staining, leading to the identification of 85 different proteins belonging to the most abundant structural and metabolic protein classes. Despite the large number of visualized spots by 2-DE, proteins with lower relative abundances, usually involved in protein biosynthesis and cell stress response, are probably masked by structural or metabolic proteins [18,19]. To counteract this, Jarrold and coworkers [14] performed the depletion of abundant muscle proteins by a high pH treatment followed by 2-DE analysis, resulting in the elimination of the major contractile proteins and in the detection of nine minor proteins, mainly belonging to mitochondria, for the first time. Nevertheless, the most often used strategy to reduce sample complexity is based on subcellular fractionation [19–21], which to our knowledge has never been done for muscle proteomics characterization.

In order to gain a deeper insight into muscle protein composition, the aim of this study was to perform the sub-cellular fractionation of gastrocnemius white portion and of soleus muscles into three different extracts: nuclear, mitochondrial/membrane, and cytosolic fractions. The validity of the proposed protocol was tested through a comparison with a commercial subcellular fractionation kit (CellLytic NuCLEAR Extraction Kit, Sigma, Munich, Germany). Comparing with the commercial kit, the methodology was improved by the introduction of three additional steps to eliminate cytoskeleton proteins from the cytosolic fraction and basic proteins from the nuclear fraction. The obtained fractions were further separated using 2-DE, with the most intense spots being excised and proteins being identified using MS data. Considering that the distribution of relative amounts of proteins on the crude extract allows only the visualization of the most abundant ones on a gel map, with this methodology we expect to improve the gel quality and the ability to load greater amounts of protein for the detection of less abundant proteins.

## Materials and methods

### Materials

IPG strips and carrier ampholytes were purchased from Amersham Biosciences (Freiburg, Germany). General chemical reagents were purchased from Roth (Karlsruhe, Germany). The protease inhibitor cocktail was supplied by Sigma.

### Preparation of tissue extracts

The experiments were performed after approval from the local ethics committee. Following the Guidelines for Care and Use of Laboratory Animals in Research, 6- to 8-week-old Charles River CD1 male mice weighing 30 to 35 g were used. The animals were housed in collective cages (2 mice/cage) and were maintained at a normal atmosphere (21–22°C, 50–60% humidity), receiving commercial food for rodents and water ad libitum in an inverted 12 h light/dark cycle. For muscle preparation, the mice were decapitated, and the white portion of gastrocnemius and the soleus muscles were dissected. These samples were quickly frozen on dry ice and stored at –80°C before use. Subcellular fractionation was performed according to Guillemin and coworkers [19] with slight modifications. Briefly, 100 mg of frozen

---

<sup>1</sup>Abbreviations used: 2-DE, two-dimensional gel electrophoresis; MS, mass spectrometry; PBS, phosphate-buffered saline; BSA, bovine serum albumin; SDS–PAGE, sodium dodecyl sulfate–polyacrylamide gel electrophoresis; MALDI–TOF, matrix-assisted laser desorption/ionization–time-of-flight; MS/MS, tandem mass spectrometry; MAP, microtubule-associated protein; OD, optical density; MLC, myosin light chain; HSP, heat shock protein.

gastrocnemius and soleus muscles (stored at  $-80^{\circ}\text{C}$ ) was transferred to 0.75 ml of buffer containing 10 mM Hepes, 10 mM NaCl, 1 mM  $\text{KH}_2\text{PO}_4$ , 5 mM  $\text{NaHCO}_3$ , 5 mM EDTA, 1 mM  $\text{CaCl}_2$ , and 0.5 mM  $\text{MgCl}_2$ . Homogenization was performed using a glass Potter–Elvehjem homogenizer. Thereafter, 100  $\mu\text{l}$  of 2.5 M sucrose was added to restore isotonic conditions for 10 min. The extract was then centrifuged at 6300g for 5 min in a tabletop centrifuge. The resultant pellet was resuspended in 0.65 ml of 10 mM Tris, 300 mM sucrose, 1 mM EDTA, and 0.1% Igepal CA-630 (v/v) at pH 7.5. This suspension was then centrifuged at 4000g for 5 min, and the resulting supernatant was discarded. This step was repeated until the supernatant was clear. The resulting pellet was resuspended in 300  $\mu\text{l}$  of 0.1 M HCl to remove the excess of basic proteins. Then it was centrifuged at 6000g for 5 min ( $4^{\circ}\text{C}$ ), and the pellet (nuclear fraction) was solubilized in 300  $\mu\text{l}$  of homogenization buffer.

The resulting supernatant from the first centrifugation was sedimented at 18,000g in a tabletop centrifuge for 150 min at  $4^{\circ}\text{C}$  (the supernatant corresponds to the cytosolic fraction). The resulting pellet (mitochondrial/membrane fraction) was solubilized in 200  $\mu\text{l}$  of homogenization buffer.

To evaluate the results obtained with the adopted protocol, we performed a subcellular fractionation using the CellLytic NuCLEAR Extraction Kit following the fabricant recommendations. Briefly, 100 mg of gastrocnemius muscle was washed twice with phosphate-buffered saline (PBS) and homogenized using a glass Potter–Elvehjem homogenizer in 1 ml of lysis buffer. The extract was centrifuged at 11,000g for 20 min (the supernatant corresponds to the cytosolic fraction). The pellet (nuclear fraction) was resuspended in 300  $\mu\text{l}$  of extraction buffer and shaken gently for 30 min. Then it was centrifuged at 20,000g for 5 min.

Total protein was estimated in all of the obtained extracts using an RC DC Protein Assay Kit (Bio-Rad, Hercules, CA, USA) with bovine serum albumin (BSA) as a standard.

## 2-DE conditions

2-DE was performed in a horizontal apparatus (IPG-phor and Hoefer 600 SE, Amersham Pharmacia Biotech, Uppsala, Sweden). Briefly, for analytical gels, 50  $\mu\text{g}$  of protein was applied onto IPG strips (13 cm, pH 3–10 NL) containing immobilines (pH 3–10 NL), 2 M thiourea, 2% Chaps, and 8 M urea. The isoelectric separation was performed using the following focusing program: 12 h at 50 mV in rehydration, 2 h at 150 V (gradient), 1 h at 500 V (gradient), 1 h at 1000 V (gradient), and 3 h at 8000 V (“step-n-hold”). After isoelectric focusing, the strip was applied on top of a sodium dodecyl sulfate-poly-acrylamide gel electrophoresis (SDS–PAGE) gel ( $12 \times 14$  cm, 12.5%), and proteins were separated according to molecular weight. The SDS–PAGE gel was stained using silver stain [22]. Spot evaluation was performed by PDQuest analysis (version 7.1, Bio-Rad). For tryptic digestion and protein identification, 350  $\mu\text{g}$  of protein was applied and the SDS–PAGE gel was stained using colloidal Coomassie blue.

## Tryptic digestion, MS analysis, and protein identification

Tryptic digestion was performed according to Detweiler and coworkers [23]. Briefly, protein spots were excised manually with a pipette tip from the gel and transferred to the Investigator ProGest automated digester (Genomic Solutions, Ann Arbor, MI, USA) rack. The gel pieces were washed twice with 25 mM ammonium bicarbonate/50% acetonitrile and dried with a nitrogen flow. Then 25  $\mu\text{l}$  of 10  $\mu\text{g}/\text{ml}$  trypsin in 50 mM ammonium bicarbonate was added to the dried residue, and the samples were incubated overnight at  $37^{\circ}\text{C}$  with sequence-grade modified porcine trypsin. Tryptic peptides were lyophilized and resuspended in 10  $\mu\text{l}$  of a 50% acetonitrile/0.1% formic acid solution. Mass spectra were obtained on a matrix-assisted laser desorption/ionization–time-of-flight MALDI-TOF/TOF mass spectrometer (4700 Proteomics Analyzer, Applied Biosystems, Foster City, CA, USA) in the positive ion reflector mode. A

data-dependent acquisition method was created to select the five most intense peaks in each sample spot for subsequent tandem mass spectrometry (MS/MS) data acquisition, excluding those from the matrix, due to trypsin autolysis or acrylamide peaks. Trypsin autolysis peaks were used for internal calibration of the mass spectra, allowing a routine mass accuracy of more than 25 ppm.

Spectra were processed and analyzed by the Global Protein Server Workstation (Applied Biosystems), which uses internal Mascot software (Matrix Science, London, UK) on searching the peptide mass fingerprints and MS/MS data. Searches were performed against the National Center for Biotechnology Information (NCBI) nonredundant protein database, and positive identifications were accepted up to 95% of confidence level.

## Results

After image analysis using the PDQuest software, the comparison of the fractions obtained by the CellLytic NuCLEAR Extraction Kit with those obtained by the proposed protocol showed an equivalent number of spots for each fraction. Comparing the observed spots for the nuclear fraction for both methodologies, a match of approximately  $75 \pm 5\%$  was achieved. The main differences were located on the basic region, where it was possible to observe, on the nuclear fraction gel map obtained with the CellLytic NuCLEAR Extraction Kit, a streak consisting of several spots (Fig. 1A). In the adopted methodology, the interference of these spots could be avoided by adding HCl before pellet solubilization. Concerning the cytosolic fraction, a match of  $65 \pm 10\%$  for the observed spots was present when the cytosolic fraction from the adopted methodology was compared with that from the CellLytic Nuclear Extraction Kit (Fig. 1). Such differences could be attributed to the separation of the cytosolic fraction into two, mitochondrial/membrane and cytosolic, using the presented methodology (Fig. 2).

### Gastrocnemius map

Using the proposed experimental protocol, the gastrocnemius silver staining nuclear and mitochondria/membrane 2-DE maps showed more than 200 spots each, and the 2-DE map of the cytosolic fraction illustrated the presence of approximately 120 spots (Fig. 2). Looking for the distribution of protein spots in the obtained 2-DE maps, it was possible to observe that the nuclear and mitochondrial/membrane fractions presented very similar spot patterns, whereas the cytosolic fraction evidenced a quite different profile.

For protein identification, 125, 80, and 65 spots were excised from the nuclear, mitochondrial/membrane, and cytosolic fractions, respectively. From these 270 excised spots, it was possible to identify 178 corresponding to 108 different proteins.

The protein identification of the nuclear fraction gel spots (Table 1) showed a bulk of structural proteins (corresponding to 47 identified spots) such as myosin light chain isoforms (spots 68A, 72A, 73A, 74A, and 75A), troponin isoforms (spots 1A, 2A, and 5A), tropomyosin (spots 55A and 56A), and actin (spots 46A and 57A). With respect to other identified protein spots, 18 belonged to metabolic pathways, 19 belonged to mitochondria pathways, 3 were related to stress response, and 22 were related to other cell functions. Among the identified proteins, it is important to emphasize the presence of the abnormal spindle (spot 9A) a microtubule-associated protein (MAP), and several proteins associated with protein biosynthesis such as the ribosomal protein L19 (spot 96A), the transcription factor c-myc protein (spot 98A), and the eukaryotic translation initiation factor 5A (spot 63A).

Examining the mitochondrial/membrane and cytosolic fractions, a number of metabolic proteins were identified and included creatine kinase (spots 21B, 22B, 23B, 46B, 47B, 15C, 17C, 21C, 28C, 38C, and 39C), phosphoglucomutase isoform 1 (spot 9B),

phosphoglucosyltransferase isoform 2 (spots 7B and 8B), and isocitrate dehydrogenase isoform 3 (spots 15B and 16B). Comparing the relative optical densities (ODs) of these two fractions, the spots corresponding to glycolytic enzymes showed high relative ODs. The sum of ODs from all identified spots of creatine kinase isoforms accounted for approximately  $16 \pm 3\%$  of the total ODs in the mitochondrial fraction and for  $22 \pm 4\%$  in the cytosolic fraction. In a similar way, aldolase isoforms accounted for approximately  $8 \pm 5\%$  in the mitochondrial fraction and for  $19 \pm 3\%$  in the cytosolic fraction.

### Soleus map

Application of the subcellular fractionation protocol to the soleus muscle yielded results similar to those for the in the gastrocnemius muscle, with the visualization of more than 200 spots in the nuclear fraction and mitochondrial/membrane fractions and approximately 110 spots in the cytosolic fraction (Fig. 3). Again, in comparing all of the obtained 2-DE maps, nuclear and mitochondrial/membrane fractions presented a strong similarity, whereas the cytosolic fraction differed substantially from the other two fractions. For the total of 310 excised spots, it was possible to identify 253 corresponding to 103 different proteins.

In the nuclear fraction, protein identification of the excised spots showed the presence of a large number of structural proteins such as actin (spots 62D and 65D), myosin light chain isoforms (spots 1D, 2D, 3D, 4D, 18D, 19D, 22D, and 32D), troponin isoforms (spots 29D, 30D, 54D, 55D, and 56D), titin (spots 40D and 41D), and des-min (spots 68D and 69D). In this fraction, it was also possible to identify a bulk of proteins related to mitochondrial functions such as NADH-ubiquinone oxidoreductase 30 kDa subunit (spot 24E), NADH-ubiquinone oxidoreductase 24 kDa (spot 26E), cytochrome c oxidase, and sub-unit VIb polypeptide 1 (spot 12E).

Results similar to those obtained in gastrocnemius for mitochondrial/membrane and cytosolic fractions were observed for soleus muscle. Hence, metabolic enzymes in cytosolic fraction, such as creatine kinase (spots 4F, 15F, 16F, 17F, 18F, 33F, 34F, and 55F), adenylate kinase 1 (spots 36F, 21F, 107F, and 89F), enolase (spots 23F, 50F, 14F, 19F, 25F, 26F, 28F, 40F, 67F, 69F, and 51F), and aldolase (24F, 39F, 49F, 54F, and 72F), accounted for approximately 42% of the total identified spots. Comparing the relative ODs of the referred enzymes, creatine kinase presented a  $7 \pm 3\%$  increase in the cytosolic fraction, and glyceraldehyde-3-phosphate dehydrogenase presented a  $6 \pm 1\%$  increase in the mitochondrial fraction.

### Comparison of gastrocnemius and soleus maps

A different protein composition profile could be observed after comparison of identified proteins in subcellular fractions of both gastrocnemius and soleus muscles. Following this, a different distribution for the structural myosin light chain (MLC) isoforms was observable when gastrocnemius and soleus muscles were compared. Gastrocnemius muscle presented one MLC1s (slow isoform) (spot 53A), one MLC1f (fast isoform) (spot 54A), two MLC2s (spots 58A and 59A), two MLC2f (spots 60A and 61A), and two MLC3f (spots 74A and 75A). Soleus muscle presented only one MLC1s (spot 19D), one MLC1f (spot 18D), one MLC2s (spot 4D), and one MLC2f (spot 3D). MS analysis of the two spots of MLC2f and MLC2s from the gastrocnemius muscle indicated that spots 59A and 61A corresponded to the phosphorylated form, whereas spots 60A and 58A corresponded to the unphosphorylated state. In the case of the soleus muscle, the unique identified spot corresponding to MLC2f was phosphorylated. A comparison of relative ODs showed a 10-fold increase for MLC1f (spot 54A) in the white gastrocnemius muscle and a 15-fold increase for MLC1s (spot 19D) in the soleus muscle. Proteins such as troponin T presented a  $9 \pm 2\%$  increase of relative ODs in the gastrocnemius muscle when compared with the soleus muscle.

Looking to the other identified proteins of both muscles, it is noteworthy to observe the number of identified spots belonging to mitochondrial redox activity such as peroxiredoxin 3, NADH-ubiquinone oxidoreductase isoforms, and cytochrome *c* oxidase. The soleus muscle presented greater relative amounts of these protein isoforms, accounting for approximately 18% of the total identified spots. Proteins belonging to the stress response class were also in greater relative amounts in the soleus muscle, accounting for approximately 9% of the total identified spots. With respect to creatine kinase and enolase, the relative ODs increased  $61 \pm 6\%$  in the gastrocnemius muscle when compared with those in the soleus muscle.

In both gel maps, we identified different spots for the same protein. This could be easily explained by the identification not only of the intact form of the protein (matching with two-dimensional *pI* and MW data) but also of fragment products of proteolytic activity and of protein aggregates. For example, regarding albumin, we found several spots corresponding to a positive identification of this protein. In the case of the gastrocnemius muscle 2-DE maps, spot 66A was identified as albumin in an intact form (sequence coverage of 27%), a form having a greater molecular mass corresponding to an albumin dimer was assigned to spot 16A (23% of sequence coverage), and spot 106A was assigned to a form of lower molecular mass corresponding to an albumin fragment (17% sequence coverage). In the case of the soleus muscle 2-DE maps, a greater number of spots were identified as albumin, covering a broad range of molecular weights corresponding to a possible dimer (spot 1F), albumin (spots 5F and 6F), and fragments (spots 60F, 78F, 68F, 8F, 111F, and 31F) covering 32% of protein sequence. Similar results were reported by Torricelli and coworkers [24], who found an albumin dimer, albumin, and albumin fragments on 2-DE maps of plasma. Considering the observed results, it is possible to suggest greater proteolytic activity regarding albumin on the soleus muscle when compared with that on the white portion of the gastrocnemius muscle.

## Discussion

In this study, we were able for the first time to present a more detailed insight into skeletal muscle proteome, especially with regard to the different functional fractions (nuclear, mitochondrial, and cytosolic). The detailed analysis of these fractions is difficult when the cytoskeletal fraction is also analyzed concomitantly, thereby masking some less expressed proteins of the other fractions by their more pronounced abundance. The currently used methodology adopted and slightly modified the protocol for subcellular fractionation described by Guillemin and coworkers [19] to refine the characterization of two types of skeletal muscles: red soleus and white portion of gastrocnemius muscles. Comparing the obtained data using the proposed experimental subcellular fractionation protocol with the CellLytic Nuclear Extraction Kit, a strong similarity between the resulting 2-DE maps was achieved. The use of this commercial kit was already advantageous for the identification of those proteins in comparison with what has been described in the literature so far [9]. The advantage of the subcellular fragmentation is based on the fact that we were able to visualize a greater number of proteins in all subcellular fractions (cf. Table 1 and Table 2). Even with this advantage, it is possible to observe a small contribution of cytoskeletal proteins such as troponin T, MLC2f, and tropomyosin in the cytosolic fraction after protein identification for the commercial kit. However, with the introduced improvements, these were absent in the data obtained with our protocol. Moreover, interference on 2-DE protein separation promoted by the contribution of basic proteins (as can be observed on the 2-DE gel map of nuclear fraction from the CellLytic Nuclear Extraction Kit [Fig. 1A]) is avoided with the current methodology. This comparison performed with the two subcellular fractionation protocols suggests that the introduced steps are advantageous for decreasing the amount of cytoskeleton and nuclear basic proteins.

Crucial steps in the methodological modifications we applied were (i) the addition of HCl to extract the basic nuclear proteins and cytoskeletal components, (ii) an additional centrifugation

to further clean the nuclear pellet, and (iii) still another centrifugation to further clean the cytosolic fraction. This way, the contribution of basic proteins, mainly histones, that tend to precipitate on the first dimension when reaching their  $pI$  [9] was depleted from the nuclear fraction. In consequence, proteins such as c-myc, eukaryotic translation elongation factor 1, and eukaryotic translation initiation factor 5A were identified for the first time in the nuclear fraction of both gastrocnemius and soleus muscles using proteomics. The additional centrifugation of the cytosolic fraction induces the reduction of cytoskeletal and mitochondrial contributions.

Comparing our data with those published previously by Gelfi and coworkers [9] and Jarrold and coworkers [14], a considerably greater number of identified proteins were achieved, amounting to 108 identified proteins in the case of the gastrocnemius muscle and to 103 in the case of the soleus muscle. Accordingly, gel maps of the nuclear fraction from gastrocnemius and soleus muscles present several spots identified as cytoskeletal components, for example, myosins, tubulin, and actin-binding proteins that constitute approximately 47% of the total number of identified proteins. Therefore, the cytosolic fractions present an enrichment in the number of observed metabolic proteins and the absence of structural proteins for both muscles. For example, the identification of parvalbumin in several spots (spots 14C, 1C, 2C, 3C, 4C, 6C, and 53C) within the cytosolic fraction from the gastrocnemius muscle, not reported previously, was possible to achieve only by using this procedure. A bulk of proteins belonging to mitochondria, covering a wide range such as for membrane composition, biosynthesis, redox activity, and metabolic pathways, were identified being distributed among nuclear and mitochondrial fractions in the gastrocnemius and soleus muscles. As described above, the pellet resulting from the first centrifugation, corresponding to the nuclear fraction, may contain a small contribution of heavy mitochondria, and this should explain the obtained results in both muscles.

The sensitivity of the current methodology also allows the detection of distinctive functional features of the different muscles under investigation. Differently expressed isoforms of proteins are the basis of muscle heterogeneity inherent to soleus and gastrocnemius muscles [10,15, 25–27]. In the current study, this was shown by the variation in the relative abundances of MLC isoforms and metabolic enzymes as well as in the presence of parvalbumin in the white portion of gastrocnemius muscle [28]. Greater amounts of MLC2f, MLC1f, and MLC3 (the latter found exclusively in gastrocnemius) were found in gastrocnemius muscle, whereas MLC1s and MLC2s were predominant in soleus muscle. Also, monophosphorylated isoforms of MLC2f and MLC2s were detected in gastrocnemius muscle. These phosphorylated forms have been described during the process of slow-to-fast transition associated with the increase of force production at low- $Ca^{2+}$  concentrations [10,29,30]. Concerning the group of metabolic enzymes, a greater expression of glycolytic enzymes, such as glyceraldehyde 3-phosphate dehydrogenase, aldolase, and enolase, was not unexpectedly found in gastrocnemius, in agreement with a greater potential in ATP production by anaerobic pathways [9,10]. On the other hand, the soleus muscle showed a greater relative abundance of carbonic anhydrase III, in agreement with its slow-twitch phenotype [9,10]. Large amounts of parvalbumin were found in the gastrocnemius muscle (several spots), in conformity with the great affinity of this protein to free  $Ca^{2+}$ , favoring the relaxation velocity enhancement that characterizes fast-twitch skeletal muscles [28,31]. We also observed differences in the expression of proteins related to cellular stress response. HSP27, HSP90, and alphaB-crystallin-related B6 were identified in the nuclear fraction of the gastrocnemius muscle, whereas HSP27, HSP70, HSP90, HSP1 (chaperonin), heat shock protein (HSP) family member 7, and cryab protein were identified in the nuclear fraction of the soleus muscle. The presence of HSP1 in soleus is in agreement with the observed overexpression of this protein shown by Golenhofen and coworkers [32] when comparing soleus with gastrocnemius. The notion of more members of the HSP family confirms the functional properties of the red soleus muscle, and this would make this muscle

more susceptible to stress conditions related to HSP as compared with the white portion of the gastrocnemius muscle. In addition, the wide range of redox proteins (found in the soleus muscle), such as NADH-ubiquinone oxidoreductase 30 kDa and 24 kDa subunits, cytochrome *c* oxidase sub-units VIb, Vb, and Va, and glutathione *S*-transferase sub-units mu1 and pi, is supportive of higher levels of oxidative enzymes in red muscle [10].

In conclusion, comparing our data with the previously published works, a significantly greater number of identified proteins were achieved, increasing to 108 identified proteins in the case of the gastrocnemius muscle and to 103 identified proteins in the case of the soleus muscle. Furthermore, these results confirm the potential of this methodology to study differential expressions of contractile proteins and metabolic enzymes, essential for generating functional diversity of muscles and muscle fiber types.

## Acknowledgment

The authors express their appreciation for the financial support provided by the “Fundação para a Ciência e Tecnologia” (FCT, grants SFRH/BPD/14968/2004 and POC-TI/QUI/5890/2004). This research was also supported in part by the Intramural Research Program of the NIH, National Institute of Environmental Health Sciences.

## References

1. Pette D, Staron SR. Cellular and molecular diversities of mammalian skeletal muscle fibers. *Rev. Physiol. Biochem. Pharmacol* 1990;116:1–76. [PubMed: 2149884]
2. Schiaffino S, Reggiani C. Molecular diversity of myofibrillar proteins: Gene regulation and functional significance. *Physiol. Rev* 1996;76:371–423. [PubMed: 8618961]
3. Booth, FW.; Baldwin, KM. Altered actin and myosin expression in muscle during exposure to microgravity *Handbook of Physiology*. Vol. 12. Bethesda, MD: American Physiological Society; 1996. p. 1075–1123.
4. Fitts HR, Riley RD, Widrick JJ. Physiology of a microgravity environment invited review: Microgravity and skeletal muscle. *J. Appl. Physiol* 2000;89:823–839. [PubMed: 10926670]
5. Pette D, Staron RS. Myosin isoforms, muscle fiber types, and transitions. *Microsc. Res. Tech* 2000;50:500–509. [PubMed: 10998639]
6. Pette D. The adaptive potential of skeletal muscle fibers. *Can. J. Appl. Physiol* 2002;27:423–448. [PubMed: 12442355]
7. Chopard A, Pons F, Marini JF. Cytoskeletal protein contents before and after hindlimb suspension in a fast and slow rat skeletal muscle. *Am. J. Physiol. Regul. Integr. Comp. Physiol* 2001;280:R323–R330. [PubMed: 11208558]
8. Yan JX, Wait R, Berkelman T, Harry RA, Westbrook JA, Wheeler CH, Dunn M. Separation and identification of rat skeletal muscle proteins using two-dimensional gel electrophoresis and mass spectrometry. *Electrophoresis* 2000;21:3666–3672. [PubMed: 11271485]
9. Gelfi C, Vigano A, De Palma S, Ripamonti M, Begum S, Cerretelli P, Wait R. 2-D protein maps of rat gastrocnemius and soleus muscles: A tool for muscle plasticity assessment. *Proteomics* 2006;6:321–340. [PubMed: 16302281]
10. Okumura N, Hashida-Okumura A, Kita K, Matsubae M, Matsubara T, Takao T, Nagai K. Proteomic analysis of slow- and fast-twitch skeletal muscles. *Proteomics* 2005;5:2896–2906. [PubMed: 15981298]
11. Isfort RJ, Wang F, Greis KD, Sun Y, Keough TW, Bodine SC, Anderson NL. Proteomic analysis of rat soleus and tibialis anterior muscle following immobilization. *J. Chromatogr* 2002;B769:323–332.
12. Cieniewski-Bernard C, Bastide B, Lefebvre T, Lemoine J, Mounier Y, Michalski JC. Identification of *O*-linked *N*-acetylglucosamine proteins in rat skeletal muscle using two-dimensional gel electrophoresis and mass spectrometry. *Mol. Cell Proteom* 2004;3:577–585.
13. Donoghue P, Doran P, Dowling P, Ohlendieck K. Differential expression of the fast skeletal muscle proteome following chronic low-frequency stimulation. *Biochim. Biophys. Acta* 2005;1752:166–176. [PubMed: 16140047]



14. Jarrold B, DeMuth J, Greis K, Burt T, Wang F. An effective skeletal muscle prefractionation method to remove abundant structural proteins for optimized two-dimensional gel electrophoresis. *Electrophoresis* 2005;26:2269–2278. [PubMed: 15880551]
15. Piec I, Lustrat A, Alliot J, Chambon C, Taylor RG, Bechet D. Differential proteome analysis of aging in rat skeletal muscle. *FASEB J* 2005;19:1143–1145. [PubMed: 15831715]
16. Le Bihan MC, Tarelli E, Coulton GR. Evaluation of an integrated strategy for proteomic profiling of skeletal muscle. *Proteomics* 2004;4:2739–2753. [PubMed: 15352248]
17. Cai D, Li M, Lee K, Wong W, Chan K. Age-related changes of aqueous protein profiles in rat fast and slow twitch skeletal muscles. *Electrophoresis* 2000;21:465–472. [PubMed: 10675029]
18. Yates JR, Gilchrist A, Howell KE, Bergeron JJ. Proteomics of organelles and large cellular structures. *Nat. Rev. Mol. Cell Biol* 2005;6:702–714. [PubMed: 16231421]
19. Guillemain I, Becker M, Ociepka K, Friauf E, Nothwang HG. A subcellular prefractionation protocol for minute amounts of mammalian cell cultures and tissue. *Proteomics* 2005;5:35–45. [PubMed: 15602774]
20. Huber LA, Pfaller K, Vietor I. Organelle proteomics: Implications for subcellular fractionation in proteomics. *Circ. Res* 2003;92:962–968. [PubMed: 12750306]
21. Abdolzade-Bavil A, Hayes S, Goretzki L, Kroger M, Anders J, Hendriks R. Convenient and versatile subcellular extraction procedure that facilitates classical protein expression profiling and functional protein analysis. *Proteomics* 2004;4:1397–1405. [PubMed: 15188407]
22. Yan JX, Wait R, Berkelman T, Harry RA, Westbrook JA, Wheeler CH, Dunn MJ. *Electrophoresis* 2000;21:3666–3672. [PubMed: 11271485]
23. Detweiler CD, Deterding LJ, Tomer KB, Chignell CF, Germolec D, Mason RP. Immunological identification of the heart myoglobin radical formed by hydrogen peroxide. *Free Radic. Biol. Med* 2002;33:364–369. [PubMed: 12126758]
24. Torricelli C, Capurro E, Santucci A, Paffetti A, D'Ambrosio C, Scaloni A, Maioli E, Pacini A. Multiple plasma proteins control atrial natriuretic peptide (ANP) aggregation. *J. Mol. Endocrinol* 2004;33:335–341. [PubMed: 15525593]
25. Gonzalez B, Negredo P, Hernando R, Manso R. Protein variants of skeletal muscle regulatory myosin light chain isoforms: Prevalence in mammals, generation, and transitions during muscle remodelling. *Pflug. Arch* 2002;443:377–386.
26. Kischel P, Bastide B, Muller M, Dubail F, Offredi F, Jin JP, Mounier Y, Martial J. Expression and functional properties of four slow skeletal troponin T isoforms in rat muscles. *Am. J. Physiol. Cell Physiol* 2005;289:C437–C443. [PubMed: 15788488]
27. Bicer S, Reiser PJ. Myosin light chain isoform expression among single mammalian skeletal muscle fibers: Species variations. *J. Muscle Res. Cell Motil* 2004;25:623–633. [PubMed: 15750847]
28. Cai DQ, Li M, Lee KK, Lee KM, Qin L, Chan KM. Parvalbumin expression is downregulated in rat fast-twitch skeletal muscles during aging. *Arch. Biochem. Biophys* 2001;387:202–208. [PubMed: 11370842]
29. Bozzo C, Stevens L, Toniolo L, Mounier Y, Reggiani C. Increased phosphorylation of myosin light chain associated with slow-to-fast transition in rat soleus. *Am. J. Physiol. Cell Physiol* 2003;285:C575–C583. [PubMed: 12748068]
30. Bozzo C, Spolaore B, Toniolo L, Stevens L, Bastide B, Cieniewski-Bernard C, Fontana A, Mounier Y, Reggiani C. Nerve influence on myosin light chain phosphorylation in slow and fast skeletal muscles. *FEBS J* 2005;272:5771–5785. [PubMed: 16279942]
31. Pauls TL, Durussel I, Cox JA, Clark ID, Szabo AG, Gagne SM, Sykes BD, Berchtold MW. Metal binding properties of recombinant rat parvalbumin wild-type and F102W mutant. *J. Biol. Chem* 1993;268:20897–20903. [PubMed: 8407923]
32. Golenhofen N, Perng MD, Quinlan RA, Drenckhahn D. Comparison of the small heat shock proteins alphaB-crystallin, MKBP, HSP25, HSP20, and cvHSP in heart and skeletal muscle. *Histochem. Cell Biol* 2004;122:415–425. [PubMed: 15480735]

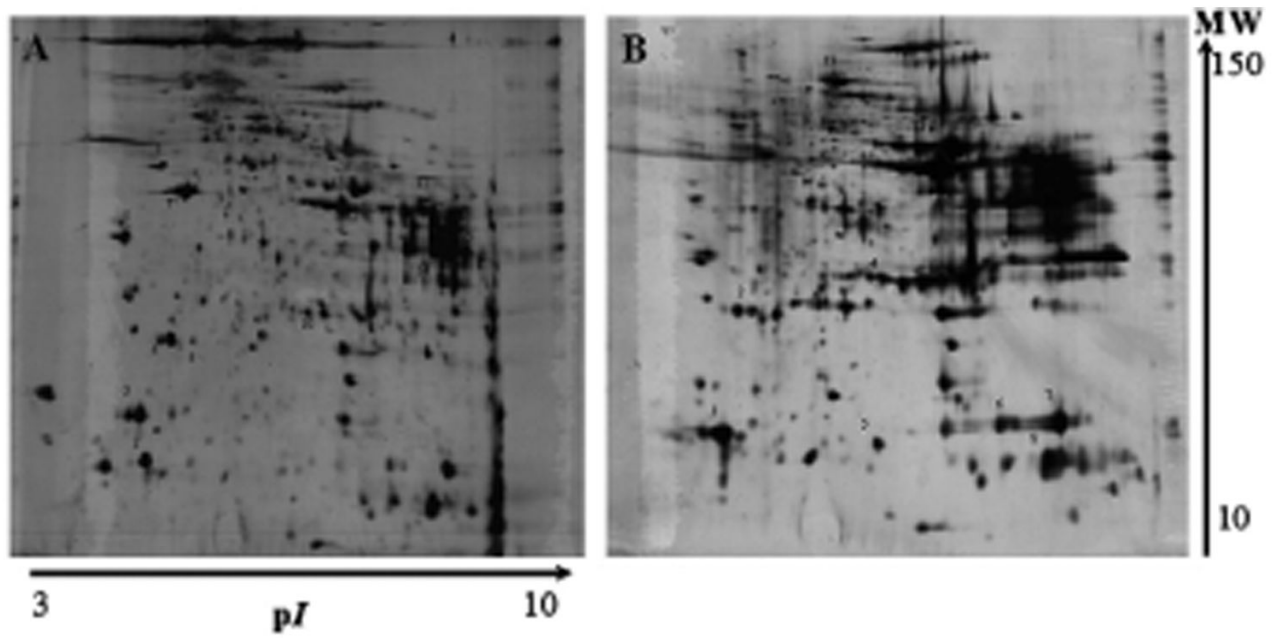


**Fig. 1.**  
2-DE representative of gastrocnemius muscle of nuclear fraction (A) and cytosolic fraction (B) obtained using the Cellytic NuCLEAR Extraction Kit.

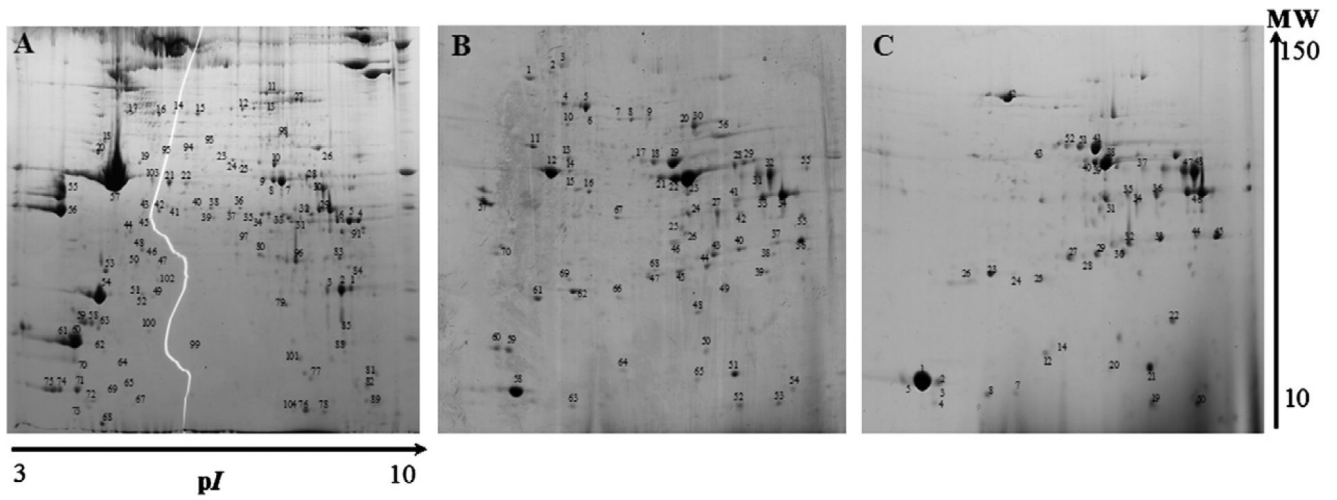


**Fig. 2.** 2-DE representative of gastrocnemius muscle of nuclear fraction (A), mitochondrial/membrane fraction (B), and cytosolic fraction (C) obtained using the adopted subcellular fractionation protocol.

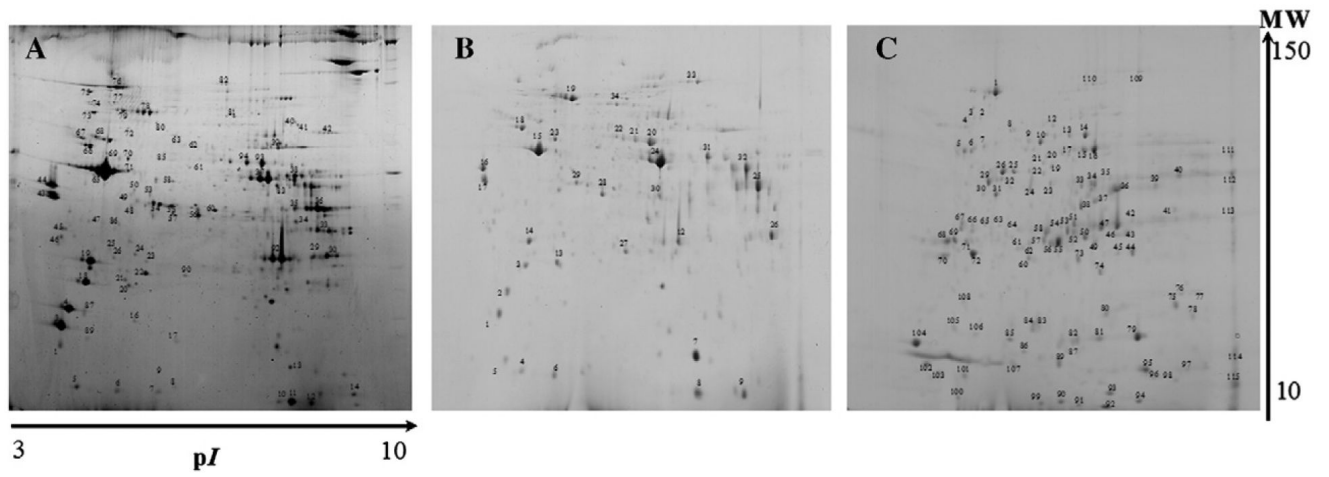


**Fig. 3.**  
2-DE representative of soleus muscle of nuclear fraction (A), mitochondrial/membrane fraction (B), and cytosolic fraction (C) obtained using the adopted subcellular fractionation protocol.

**Table 1**  
 Identified gastrocnemius muscle proteins in nuclear, mitochondrial/membrane, and cytosolic fractions

Gastrocnemius muscle		Fraction						
Protein identification	Accession number	MW	Nuclear	Mit/Mem	Cytosol	Previous work	Spot(s)	
13K protein	191493	13502		X	X		54B, 25C	
14-3-3 protein gamma	3065929	28345		X		g	70B	
Abnormal spindle	34880454	364239	X				9A	
Actin	55577	42024	X			g	46A, 57A, 94A, 21A, 103A	
Actinin alpha 3	7304855	102978		X		g	3B	
Adenylate kinase 1	10946936	23106	X	X	X	g	23C, 52C, 51 A, 36B	
Albumin	55391508	68714	X	X	X	g	22C, 66A, 16A, 106A, 5B	
Aldolase A	7548322	39526	X	X	X	g	97A, 29A, 31B, 42B, 13C, 20C, 35C, 36C, 37C, 47C, 48C	
Alpha globin 2	16973681	15193	X				104 A	
Alpha-actin (aa 40-375)	49864	37788	X	X			48A, 19A, 45A, 62A, 12B	
Alpha-fetoprotein	191765	47195			X		42C, 27C	
Alpha-globin	553919	12899	X	X	X		50C, 78A, 53B	
Apolipoprotein A-I precursor	109571	30358	X	X			50A, 69B	
ATP synthase, H+ transporting mitochondrial F1 complex, beta subunit	31980648	56265	X	X		g	20A, 49B	
ATP synthase, H+ transporting, mitochondrial F0 complex, subunit F	7949005	12489	X				52A, 67A	
ATP synthase, H+ transporting, mitochondrial F1 complex, alpha subunit, isoform 1	6680748	59716	X	X		g	26A, 56B	
ATP synthase, H+ transporting, mitochondrial F1 complex, O subunit	20070412	23349	X				84A	
Beta-1-globin	4760590	15699	X				76A	
Capping protein (actin filament) muscle Z-line, alpha 2	38322760	32947	X				43A	
Carbonic anhydrase 3	31982861	29348	X	X		g	43B, 80A	
Chain D, Chimeric Mouse carbonmonoxy hemoglobin	18655689	15607		X			52B	
Citrate synthase	13385942	51703	X				30A	

Gastrocnemius muscle		Fraction						
Protein identification	Accession number	MW	Nuclear	Mit/Mem	Cytosol	Previous work	Spot(s)	
C-myc protein	37933209	21304	X				98A	
Cofilin 2, muscle	6671746	18698	X			g	101A	
Creatine kinase, muscle	6671762	43018	X	X	X	g	7A, 28A, 8A, 9A, 31A, 35A, 25A, 66A, 21B, 22B, 23B, 24B, 26B, 46B, 47B, 65B, 12C, 17C, 21C, 28C, 38C, 39C	
Cryab protein	14789702	20056	X	X			79A, 48B	
Cu/Zn superoxide dismutase	226471	15752		X	X		64B, 19C	
Cytochrome c oxidase subunit Va preprotein	55971	16119	X				70A	
Cytochrome c oxidase, subunit Vb	6753500	13804	X				99A	
Cytochrome c, somatic	6978725	11598	X				81A	
Desmin	1352241	53073	X	X		g	20A, 11B	
Dihydrolipoamide S-acetyltransferase precursor	16580128	59047		X			6B	
DnaK-type molecular chaperone	109414	70761		X		g	4B	
Enolase 1, alpha non-neuron	54673814	47111	X				23A	
Enolase 3, beta	54035288	46984	X	X	X	g	10A, 18B, 31C, 41C	
Eukaryotic translation initiation factor 5A	56800106	16292	X				63A	
Expressed in non-metastatic cells 2	56270600	17352		X			50B	
Fast myosin alkali light chain	13487933	16603	X				54A, 72A	
Fast skeletal muscle troponin C	6678371	18098	X				90A	
Fatty acid binding protein 3	54306426	10931	X			g	65A	
Fatty acid binding protein 3, muscle and heart	6753810	14810		X	X		64B, 5B	
Glutathione S-transferase, mu 1	6754084	25953		X			38B	
Glutathione S-transferase, pi	25453420	23424		X			39B	
Glyceraldehyde-3-phosphatedehydrogenase	55154587	35787		X		g	33B, 34B	
Glyceraldehyde-3-phosphate dehydrogenase (phosphorylating) (EC 1.2.1.12)	51769013	35807			X		41B, 35B, 33C, 44C, 45C	
Glycerol-3-phosphate dehydrogenase 1	13543176	36934		X			11B	
Heat shock 90kDa protein 1, beta	51859516	83289		X		g	1B	

Gastrocnemius muscle									
Fraction									
Protein identification	Accession number	MW	Nuclear	Mit/Mem	Cytosol	Previous work	Spot(s)		
Heat shock protein 27	204665	22879	X				47A		
Heat shock protein, alpha-crystallin-related, B6	59808419	17510	X				100 A		
Isocitrate dehydrogenase 3 (NAD+) alpha	18250284	39613		X		g	15B, 16B		
Kelch-like 20	31542490	67369	X			g	43A		
Lactate dehydrogenase 1	13529599	34481	X			g	33A		
Lactate dehydrogenase 1, A chain	6754524	36475		X		g	27B		
Lectin, galactose binding, soluble 1	12805209	14868			X		8C		
Malate dehydrogenase 1, NAD (soluble)	15100179	36460		X		g	67B		
Mitochondrial aconitase	10637996	85421	X				27A		
Mitq-like protein	1401252	8509	X				89A		
Muscle glycogen phosphorylase	6755256	97225	X				11 A, 12A		
Myoglobin	21359820	17059	X			g	77A, 5 1B		
Myosin A1 catalytic light chain, skeletal muscle	91114	20580	X				58A		
Myosin A2 catalytic light chain, skeletal muscle	91115	16588	X				64A, 74A		
Myosin light chain 1 slow a	26986555	22735	X				49A, 53A		
Myosin light chain 2v	38511915	18780	X			g	60A, 59B		
Myosin light chain, phosphorylatable, fast skeletal muscle	7949078	18943	X	X			61A, 68A, 69A, 73A, 60B		
Myosin, heavy polypeptide 4, skeletal muscle / similar to myosin heavy chain 2b	56206252	230720	X			g	14A		
Myosin, light polypeptide 1	29789016	20581	X	X		g	61B		
Myosin, light polypeptide 3	6981240	22142	X			g	74A, 75A		
NADH dehydrogenase (ubiquinone) 1 alpha subcomplex 10	13195624	40578	X			g	24A		
NADH dehydrogenase (ubiquinone) Fe-S protein 2	23346461	52952	X			g	22A		
NADH dehydrogenase (ubiquinone) Fe-S protein 3	20071222	30187	X				47A		
NADH dehydrogenase 1 beta subcomplex 4	21314826	15072	X				88A		
Orf	5441500	31432	X				85A		
Oxoglutarate dehydrogenase (lipoamide)	33563270	116043	X				13A		

Gastrocnemius muscle									
Fraction									
Protein identification	Accession number	MW	Nuclear	Mit/Mem	Cytosol	Previous work	Spot(s)		
Parvalbumin	30352200	11236			X		14C, 1C, 2C, 3C, 4C, 52C, 70A, 71A, 58B		
Pdlim7 protein	30931151	24643	X				86A		
PDZ and LIM domain 5 isoform ENH2	11602914	36034	X			g	83A		
PDZ-LIM protein cypher2s	11612598	31408	X				91A		
Peroxiredoxin 3	6680690	28109	X				102A		
Phosphatidylethanolamine binding protein	53236978	20817			X	g	26C		
Phosphoglucosyltransferase 1	8393951	61365		X		g	9B		
Phosphoglucosyltransferase 2	31980726	61479		X			7B, 8B		
Phosphoglycerate kinase 1	40254752	44510		X		g	28B, 29B		
Phosphoglycerate mutase 2	9256624	28809		X			25B, 37B, 40B		
Polyubiquitin	1050930	11234			X		18C, 46C		
Pyruvate dehydrogenase (lipoamide) (EC 1.2.4.1) beta chain	112253	38823	X			g	44A		
Pyruvate kinase, isozyme M2	2506796	57850		X		g	20B, 30B, 98A		
Ribosomal protein L19	6677773	23467	X				96A		
Sarcolumenin	34328417	99123	X				93A, 95A		
Sarcomeric mitochondrial creatine kinase	57537	47355	X				28A		
Sdha protein	15030102	72280	X				15A		
Serpina1a protein	15929675	45593			X		55C		
Slow skeletal muscle troponin T2	33465564	31067	X				41A		
Slow skeletal muscle troponin T3	33465568	29862	X				42A		
Sod2 protein	17390379	24070		X			68B		
Superoxide dismutase 1, soluble	56270595	15933			X		10C		
Transferrin	56541070	15766			X		43C		
Triosephosphate isomerase	1864018	22492			X		9C, 34C		
Triosephosphate isomerase 1	6678413	26696		X		g	45B, 49B, 40C		
Tropomyosin 2, beta	11875203	32817	X				55A		
Tropomyosin alpha chain, striated muscle	92921	32693	X	X		g	56A, 57B		
Troponin I, skeletal, fast 2	6678391	21344	X			g	1A, 2A, 3A, 86A, 87A		



Gastrocnemius muscle		Fraction						
Protein identification	Accession number	MW	Nuclear	Mit/Mem	Cytosol	Previous work	Spot(s)	
Troponin T	2340050	28320	X				5A, 17A, 32A, 34A, 36A, 37A, 39A, 40A, 4A, 6A, 38A	
Ubiquinol-cytochrome c reductase binding protein	21595014	13601	X			g	82A	
Ubiquinol-cytochrome-c reductase complex core protein I, mitochondrial precursor	14548301	52735		X			13B	
Valosin-containing protein	17865351	89293		X			2B	
Voltage-dependent anion channel 1	13786200	30737	X			g	42A	
Periredoxin 6						g		
Dj-1						g		
Malate dehydrogenase						g		
Arsenical pump						g		
Myosin-binding protein H						g		
Aspartate aminotransferase						g		
haptoglobin						g		
Dihydrolipoylysine-residue acetyltransferase component of pyruvate						g		
Dehydrogenase complex						g		
Creatine kinase, sarcomeric mitochondrial						g		
Glycogen phosphorylase						g		
Serotransferrin						g		
Nucleoside diphosphate kinase B						g		
Alpha crystallin B chain						g		
Cathepsin D						g		
ATP synthase D chain,						g		
Annexin A6						g		
Hsp70						g		
Succinyl-CoA						g		
Mitochondrial inner membrane protein						g		
Dihydrolipoylysine-residue						g		

Gastrocnemius muscle		Fraction						
Protein identification	Accession number	MW	Nuclear	Mit/Mem	Cytosol	Previous work	Spot(s)	
Succinyltransferase component of 2-oxoglutarate dehydrogenase complex, mitochondrial						g		
Heat-shock protein beta-6						g		
CAPZb protein						g		
Adenosine kinase						g		
Gelsolin						g		
Dihydropyrimidine dehydrogenase, mitochondrial						g		
Glyoxalase 1						g		
Aconitate hydratase, mitochondrial						g		
Succinyl-CoA ligase [ADPforming] beta-chain, mitochondrial						g		

*Note.* Mit/Mem, mitochondrial/membrane. In the "previous work" column, the letter "g" refers to Ref. [9].

**Table 2**  
Identified soleus muscle proteins in nuclear, mitochondrial/membrane, and cytosolic fractions

Soleus muscle		Fraction						
Protein identification	Accession number	MW	Nuclear	Mit/Mem	Cytosol	Previous work	Spot(s)	
Aconitase 2, mitochondrial	18079339	85410			X		109F, 110F	
Actin	55577	42024	X	X	n		15E, 42D, 52D, 65D	
Actin-capping protein beta chain, splice form 1	1083244	31326	X				86D	
Acyl-CoA dehydrogenase (EC 1.3.99.3) precursor, short-chain-specific, mitochondrial	2137773	44918	X				59D	
Adenylate kinase 1	15928666	21526			X		107F, 89F, 21F, 36F	
Albumin	55391508	68714	X	X	X	n	1F, 5F, 6F, 60F, 78F, 68F, 8F, 111F, 3 1F, 78D, 19E	
Aldolase A	7548323	39526	X		X		24F, 39F, 49F, 54F, 72F, 83D	
Alpha-actin (aa 40–375)	49864	37788	X				49D	
Alpha-fetoprotein	191765	47195			X		7F, 9F, 2F, 10F, 58F	
Ankyrin repeat domain 2	9910130	36684	X				53D	
Apolipoprotein B editing complex 2	6753098	25644	X				44D	
ATP synthase, H+ transporting mitochondrial F1 complex, beta subunit	31980648	56265	X				66D	
ATP synthase, H+ transporting, mitochondrial F0 complex, subunit d	51980458	18738	X	X			20D, 21D, 13E	
ATP synthase, H+ transporting, mitochondrial F1 complex, alpha subunit, isoform 1	6680748	59716	X		X		59F, 39D	
ATP-specific succinyl-CoA synthetase beta subunit	3766201	46215	X				71D	
Beta tubulin	537407	49716	X				67D	
Beta-I-globin	4760590	15699	X		X		10D, 95F	
Beta-tropomyosin	50190	32925		X			16E, 17E, 44D	
Carbonic anhydrase 3	31982861	29348	X	X	X	n	38F, 46F, 47F, 61F, 91F, 93F, 12E, 92D	
Chain D, Chimeric Mouse carbonmonoxy hemoglobin	18655689	15607			X		63F, 90F	

Soleus muscle		Fraction						
Protein identification	Accession number	MW	Nuclear	Mit/Mem	Cytosol	Previous work	Spot(s)	
Creatine kinase, muscle	6671762	43018	X	X	X		4F, 16F, 76F, 15F, 17F, 33F, 34F, 55F, 79F, 96F, 98F, 106F, 4E, 9D	
Cryab protein	14789702	20056	X		X		15D, 74F	
Cu/Zn superoxide dismutase	226471	15752			X		84F	
Citrate synthase	13385942	51703	X				37D	
Cytochrome c	34871328	11628	X				14D	
Cytochrome c oxidase, subunit Va	6680986	16020	X	x			5D, 5E, 6D, 6E	
Cytochrome c oxidase, subunit Vb	6753500	13804	X	x			8D, 8E	
Cytochrome c oxidase, subunit Vfb polypeptide I	19353360	10065	X				12D	
Desmin	33563250	53465	x			n	68D, 69D, 18E	
Dihydrolipamide S-acetyltransferase precursor	16580128	59047	X				79D	
DJ-1 protein	55741460	20008			X		13E	
DnaK-type molecular chaperone	109414	70761	X				77D	
Electron transfer flavoprotein beta-subunit (Beta-ETF)	21759114	27293			X		113F	
Electron transferring flavoprotein, alpha polypeptide	13097375	35018			X		37F	
Enolase 1, alpha non-neuron	54673814	47111			X		11F	
Enolase 3, beta	54035288	46984	x	x	x		14F, 19F, 25F, 26F, 40F, 5 1F, 67F, 69F, 20E, 21E, 22E, 93D, 94D	
Eukaryotic translation elongation factor 1 gamma	53237111	50029			X		62D	
Expressed in non-metastatic cells 2	55778652	17272			X		80F	
Fast myosin alkali light chain	13487933	16603	X				1D	
Fatty acid binding protein 3	54306426	10931			X		103F	
Fatty acid binding protein 3, muscle and heart	6753810	14810	X		X		7D, 12F	
Fibrinogen, B beta polypeptide	33859809	54718	X				80D	
FLJ12649 protein	39963533	89971	X				47D	
Glyceraldehyde-3-phosphate dehydrogenase (phosphorylating) (EC 1.2.1.12)	51764212	35789				n	35D, 75F, 92F	

Soleus muscle		Fraction						
Protein identification	Accession number	MW	Nuclear	Mit/Mem	Cytosol	Previous work	Spot(s)	
Heat shock 27kDa protein 1	57086605	22808	X				27D	
Heat shock 70kD protein 5	25742763	73202	X				74D	
Heat shock 90kDa protein 1, beta	51859516	83289	X				75D	
Heat shock protein 1 (chaperonin)	31981679	60918	X				72D	
Heat shock protein family, member 7	31542970	18623	X				60D	
Heat shock protein HSP27	424145	21961	X				25D	
heat shock protein, alpha-crystallin-related, B6	59808419	17510	X				16D, 88D	
Hemoglobin alpha chain	49900	15079			X		29F, 11D, 94F	
Hspb1 protein	17390597	23000	X				23D	
Isocitrate dehydrogenase 2 (NADP+), mitochondrial	37748684	50874	X	X			45F, 38D, 3 IE	
Isocitrate dehydrogenase 3 (NAD+) alpha	18250284	39613	X				50D, 5 1D	
LOC434246 protein	45500997	41182	X				63D	
Malate dehydrogenase 1, NAD (soluble)	15100179	36460		X	x		32F, 87F, 73F, 53F, 108F, 34E	
Malate dehydrogenase, mitochondrial	42476181	35661	X	X			25E, 36D, 112F	
Muscle-specific enolase beta subunit	387144	40680			X		50F, 23F	
Myoglobin	21359820	17059		X		n	7E, 9E, 13D, 85F, 81F	
Myosin A1 catalytic light chain, skeletal muscle	91114	20580	X				87D	
Myosin light chain 1 slow a	26986556	22735	X	x		n	18D, 3E, 22D, 19D, 14E	
Myosin light chain, phosphorylatable, fast skeletal muscle	7949078	18943	X	x		n	4D, 2E	
Myosin light chain 3, skeletal muscle isoform (A2 catalytic) (Alkali myosin light chain 3) (MLC3F)	127134	16589	X			n	18D	
Myosin light chain, phosphorylatable, fast skeletal muscle	7949078	18943	X	x			3D, 1E	
NADH dehydrogenase (ubiquinone) 1 alpha subcomplex 10	13195624	40578	X				58D	
NADH dehydrogenase (ubiquinone) Fe-S protein 1	21704020	79698	X				76D	
NADH dehydrogenase (ubiquinone) Fe-S protein 2	23346461	52592	X				85D	
NADH dehydrogenase (ubiquinone) flavoprotein 2	51770347	28852	X				31D	

Soleus muscle		Fraction						
Protein identification	Accession number	MW	Nuclear	Mit/Mem	Cytosol	Previous work	Spot(s)	
NADH-ubiquinone oxidoreductase 24 kDa subunit, mitochondrial precursor	20178012	27298	X				26D	
NADH-ubiquinone oxidoreductase 30 kDa subunit, mitochondrial precursor (Complex I-30(KD))	23396786	30189	X				24D	
Nexilin isoform s	40538878	78345			X		32F	
Oxoglutarate dehydrogenase (lipoamide)	56206143	117682	X	X			33E, 82D	
Parvalbumin	30352200	11236			X		102F, 104F	
PDZ-LIM protein cypher2s	11612598	31408	X				90D	
Peroxiredoxin 3	6680690	28109	X				28D	
Peroxiredoxin 6	6671549	24811			X		57F	
Phosphatidylethanolamine binding protein	53236978	20817			X		70F	
Phosphoglycerate mutase 2	9256624	28809	X				17D	
Pyruvate dehydrogenase (lipoamide) (EC 1.2.4.1) beta chain	112253	38823	X				48D	
Pyruvate kinase, isozyme M2	2506796	57850			X		22F	
Sarcomeric mitochondrial creatine kinase	57537	47355	X				84D	
Similar to hypothetical protein	55625512	20177	X				89D	
Similar to Kelch repeat and BTB domain containing protein 10 (Kelch-related protein 1) (Kel-like pr)	38074800	68147	X				73D	
Slow skeletal muscle troponin T 2	33465568	29862			X		28E	
Slow skeletal muscle troponin T 3	33465568	29862			X		54D, 55D, 29E	
Succinate dehydrogenase Fp subunit	15030102	72280	X				81D	
Superoxide dismutase 2, mitochondrial	31980762	24588			X		44F	
Titin immunoglobulin domain protein (myotilin)	10946892	55282	X				40D, 4 1D	
Triosephosphate isomerase	1864018	22492			X		62F, 56F, 43F	
Troponin I isoform	1082876	28403	X			n	43D	
Troponin I, skeletal, fast 2	6678391	21344	X	X			29D, 26E, 30D	
Troponin T	2340050	28320	X				56D, 57D	
Tu translation elongation factor, mitochondrial	27370092	49477	X				61D	
Tyrosine 3-monooxygenase/tryptophan 5-monooxygenase activation protein, epsilon polypeptide	31981925	29170	X				45D	

Soleus muscle	Fraction							
	Protein identification	Accession number	MW	Nuclear	Mit/Mem	Cytosol	Previous work	Spot(s)
Ubiquinol-cytochrome-c reductase complex core protein I, mitochondrial precursor	14548301	52735			X			23E, 70D
Voltage-dependent anion channel 1	13786200	30737	X					33D, 34D
Glycogen phosphorylase b							n	
Filamin, muscle isoform							n	
b-MHC							n	
MHC, 2x							n	
b-MHC							n	

*Note.* Mit/Mem, mitochondrial/membrane. In the "previous work" column, the letter "n" refers to Ref. [10].